Chapter 3

Mechanism of Intra-molecular Hydrogen Bonding Formation in Phenolic Analogue Models and their Structural Analysis

3.1 Background

As previously discussed, it was found that linear structured p-cresol/ formaldehyde (PCF) resins have much stronger hydrogen bonds than those found in ordinary branched-structured phenolic resins, i.e., resol and novolac. The former unbranched polymer exhibits an unusual thermal transition due to intra-molecular hydrogen bonding in the form of "calixarene-like" structures, which cannot be formed in the branched structures of the latter. When heated up to a transition temperature, the "calixarene-like" structure in PCF is destroyed and apparently largely replaced by intermolecular hydrogen bonding. Once destroyed, the cyclic structure cannot be recovered by simply cooling down or annealing. However, the original structure can be obtained by dissolving and recasting the sample from solution. This suggests that in these materials there is an interesting coupling of the conformational freedom of the chains with intra- and intermolecular interactions.

In this chapter, the nature of hydrogen bonding formed between phenolic hydroxyls is examined by employing infrared spectra of two low molar mass phenolic analogues; bis-2-hydroxyphenylmethane (B2HPM), and bis-4-hydroxyphenylmethane (B4HPM). FTIR spectra of these two compounds in dilute solutions of cyclohexane (CHEX) solvent as a function of concentration is recorded. In addition, structural analysis is conducted to investigate structural conformation of the compounds by applying ab-initio calculations. B2HPM was used to represent the linear structure of PCF whose all OH groups are located at *ortho*- positions relative to the methylene linkage. B4HPM, on the other hand, consists of phenolic dimer whose hydroxyl groups are separated by phenolic rings, as the groups are placed at *meta*- positions relative to the methylene (See Figure 3.1). The latter structure was employed to represent branch-structured phenolic resin. Less complicated band patterns in the infrared spectra of these model compounds provides important information on hydrogen bonding formation and related conformational structures, which can be used to explain the corresponding phenomena observed in phenolic resins.

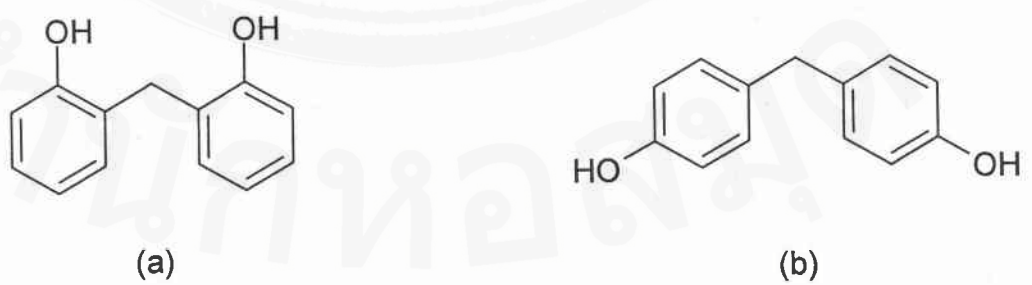

Figure 3.1 Chemical structures of B2HPM (a), and B4HPM (b).

The infrared spectra in solid phase of the two low-molecular weight analogues, B2HPM and B4HPM, are first examined as shown in Figure 3.2. Essentially, 2% of the model compounds are homogeneously mixed with KBr powder and pressed into a pellet. The spectra, in the OH-stretch region, are complex but show significant difference in the nature of hydrogen bond between the two models. The spectrum of B4HPM shows a "free" OH stretching mode at 3562 cm^{-1}, and intensely overlapped hydrogen bonded-OH vibrational modes at 3420, 3344, and 3276 cm^{-1}, respectively. These are probably associated with a distribution of dimer, trimer, and multimers hydrogen bonding. The corresponding spectrum of B2HPM, however, exhibits hydrogen bonded OH stretching bands at 3402, 3316, and 3257 cm^{-1}, respectively, which are slightly lower in frequency compared to those observed in B4HPM. More importantly, vibrational mode due to "free" OH stretching is diminished in the spectrum of this model compound, compared to that observed in the B4HPM counterpart. This indicates that the majority of hydroxyl groups in B2HPM are hardly present in "free" state. Also, as the functional groups are in close proximity, this enable the OH to form stronger intramolecular hydrogen bonding, in addition to intermolecular hydrogen bonds. This is reflected by the shift to lower wavenumber of the overall hydroxyl bands, compared to that of B4HPM where majority of the hydroxyls are probably intermolecular hydrogen bonded. These results from solid phase samples exhibit infrared characteristics that are parallel to those observed in phenolic resins.

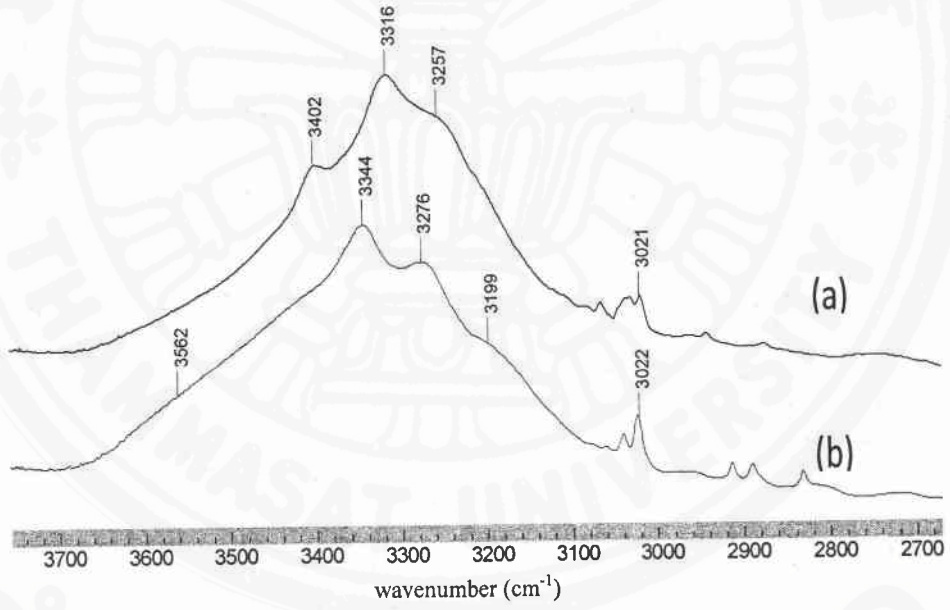

Figure 3.2 FTIR spectra in a solid phase of B2HPM (a), and B4HPM (b).

3.2 FTIR Study of Dialogue Model in Dilute Solutions

We now examine the nature of the two model compounds in dilute solutions. Anhydrous cyclohexane (CHEX) was employed as it is an inert solvent and exhibits minimum number of peaks in the hydroxyl stretching region. Dilute solution of the model compounds were prepared, and their FTIR spectra were subsequently recorded by using a sealed KBr liquid cell with a path length of 1.0 mm. The vibration patterns of hydroxyl groups of the analogues were investigated by subtracting the spectrum of pure CHEX

from that of the model's dilute solutions. The resulting infrared spectra after subtraction obtained from B4HPM and B2HPM are shown in Figure 3.3 and Figure 3.4, respectively. The different spectra of B4HPM solutions show a single band located at 3597 cm^{-1}, whose frequency is independent on the concentration. The band intensity is, however, increasing as a function of concentration (concentrations vary from 5×10^{-3} to 1×10^{-3} M). This band is therefore assigned to the vibration of "free" OH groups, reflecting that beyond this range of concentration the probability of the hydroxyls forming intermolecular hydrogen bonding is negligible, as the trace amount of the compound are separated by a large excess volume of the inert solvent. A formation of intramolecular hydrogen bonding is also unlikely (at any concentrations), as the two hydroxyl groups are completely isolated by the non-polar phenolic rings.

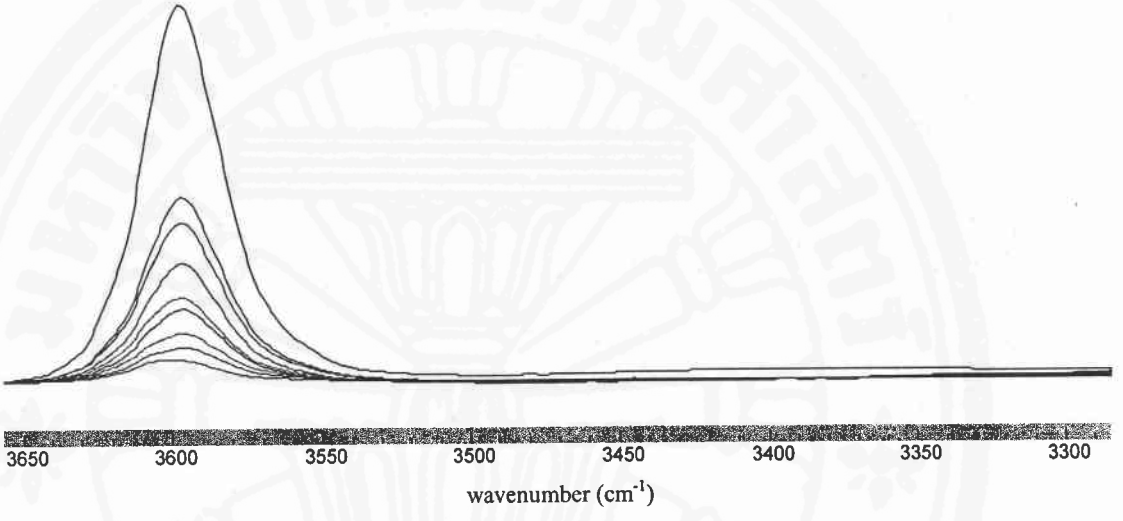

Figure 3.3 Infrared characteristic of OH groups in B4HPM as a function of solution concentrations.

Corresponding measurements were also conducted on B2HPM. A series of dilute solutions in the range of 7×10^{-3} to 7×10^{-4} M were prepared and their infrared spectra were recorded. The resulting spectra after subtraction of a pure CHEX spectrum, as shown in Figure 3.4, exhibits different band patterns (in the hydroxyl stretching region) to that previously discussed in B4HPM. Three well-resolved bands are observed at 3609, 3483, and 3307 cm^{-1}, respectively. The first band is assigned to "free" OH, as its frequency is comparable to that observed in B4HPM. The slight shift in the frequency to higher wavenumber might be due to weak interaction between the hydroxyl groups and the hydrogen atoms of methylene group. This O··H-C hydrogen bonding is, in turn, strengthen the O-H bond, resulting in a blue shift in FITR spectrum. A similar interaction cannot be observed in B4HPM, whose methylene Hydrogens are not in close-proximate to the hydroxyl groups.

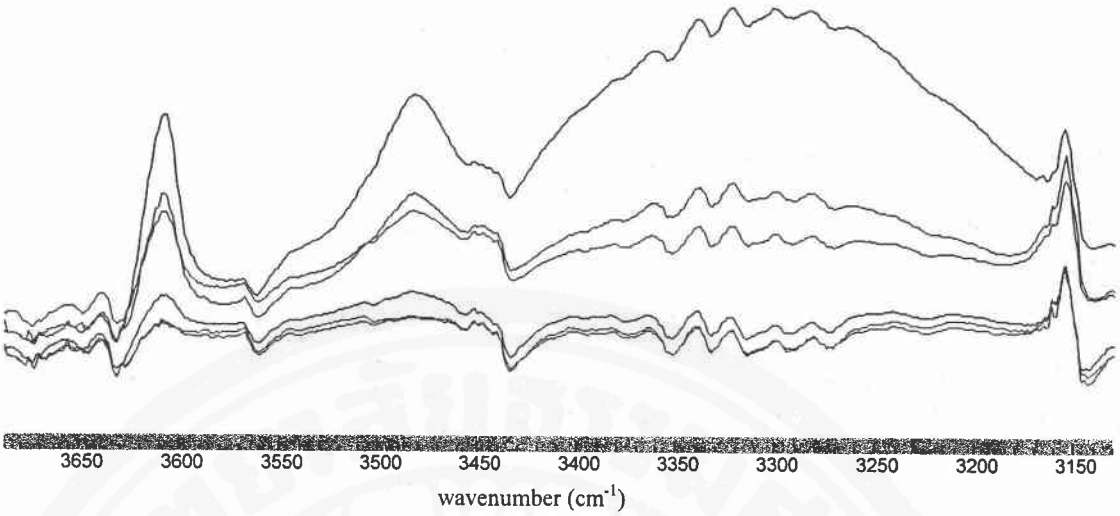

Figure 3.4 Infrared characteristic of OH groups in B2HPM as a function of solution concentrations.

The latter two vibrational modes are clearly corresponding to hydrogen bonded OH, as indicated by their lower frequencies. The former mode is assigned to intra-molecular hydrogen bonded OH stretching, as a result from the close proximate between the two hydroxyl groups from the adjacent phenolic rings. This agrees with the intensity ratio of the corresponding two bands, which is significantly independent of concentration. Intriguingly, the latter band (3307 cm^{-1}) shows a large redshift from the free OH vibration, indicating a formation of stronger hydrogen bonding patterns. This vibrational mode is probably due to intermolecular hydrogen bonded OH observed when two or more units of B2HPM interacting and forming structural conformation. It is interesting to observe this hydrogen bonded pattern in B2HPM but not B4HPM, even though the two solutions were prepared in comparable concentration range. Moreover, the intensity ratio of this hydrogen bonded OH and the free OH band is concentration dependent, unlike those found in the former band. These results significantly indicate that the existent of intra-molecular hydrogen bonding pattern (as a result of close proximities of OH groups) induce a formation of "dimmer" or "trimer" B2HPM structural conformations by employing intermolecular hydrogen bonding. Peak fitting was also applied to determine band area of the three OH stretching bands. Data of band area from the three modes can be examined as a function of concentration to obtain equilibrium constant of the hydrogen bonding formation. However, due to space limitation, this will not be discussed here.

3.3 Structural Analysis of Analogue Models

Turning now to molecular geometry calculations, structural analysis by employing DFT calculations was conducted. Essentially, the initial conformations of B2HPM and B4HPM were constructed by GaussView 2.08 program. Structures analysis was performed in the gas phase by Gaussian 03 software package running on a 3 GH_z processor of a Dell model Optiplex GX260 mini tower computer. The geometries of B2HPM and B4HPM were fully optimized with an ab initio method, HF/3-21G(d,p) basis set. The minimum

energy conformation of compounds was used as a starting structure in the torsional potentials ab initio calculations of the dihedral angles given by the carbon-oxygen single bonds.

The results of torsion angle α rotational potential of B4HPM, as shown in Figure 3.5, provide minima with only slightly energy difference (0.01-0.14 kJ/mol). This low value of energy difference suggests that there is no favorable structural conformation in B4HPM. This, in turn, reflects an absent of specific interaction, i.e., hydrogen bonding, in all possible structural conformations of this model compound. On the other hand, the energies relative to the α torsion angle of B2HPM, as shown in Figure 3.6, indicate two minima at α = -90° and 90°, respectively. The energy difference between the two structural conformations is 15.7 kJ/mol and the activation barriers are 47.52 and 15.15 kJ/mol, respectively. The results indicate that the global energy minimum conformation is obtained when intramolecular hydrogen bonding formation is achieved, as shown in the molecular structure in Figure 3.6. However, the structure of the second minimum conformation at α = 90° indicates that the two hydroxyl groups are placed on the opposite side of phenolic rings, inhibiting a formation of hydrogen bonding. The barrier energy between the two minima indicate that intramolecular hydrogen bonding between the two adjacent hydroxyl groups is a driving force for the existence of the global minimum conformation. Two-dimensional energy surface as obtain by HF/3-21G(d,p) calculations is shown in figure 3.7. The results from this calculation are in good agreement with those observed in FTIR experiment and our band assignment.

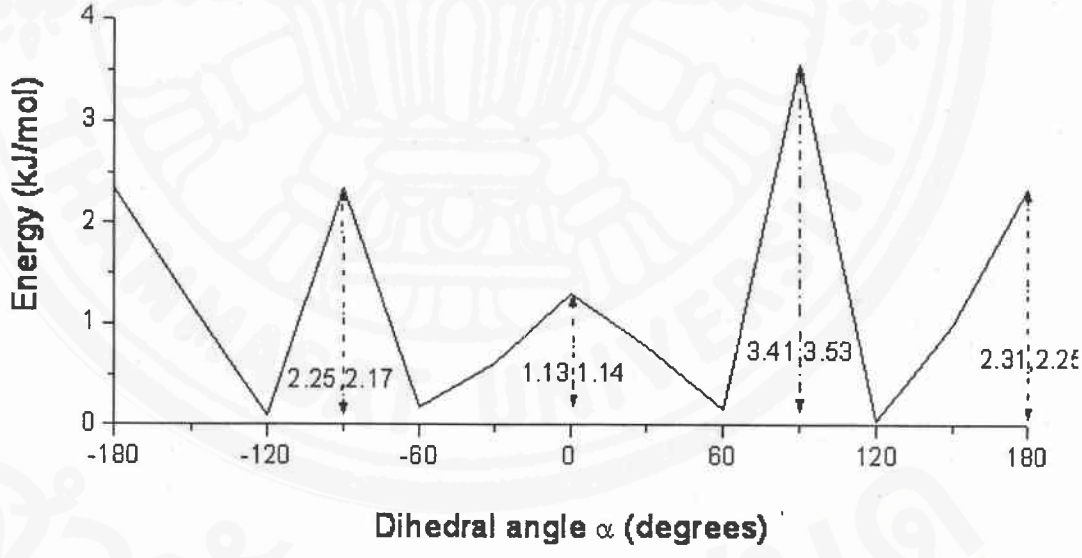

Figure 3.5 Rotational potential of the dihedral angle α of B4HPM.

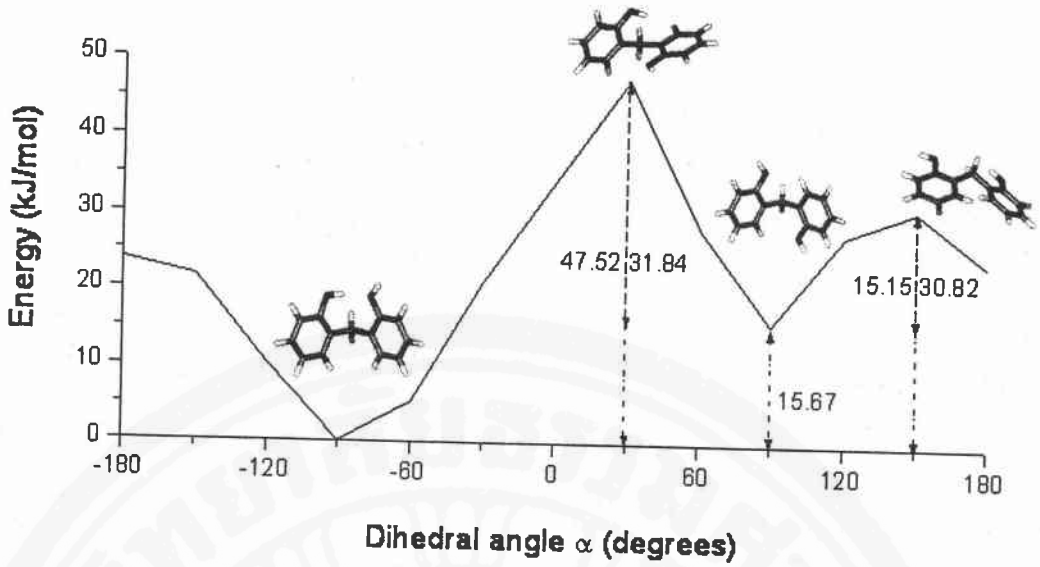

Figure 3.6 Rotational potential of the dihedral angle α of B2HPM.

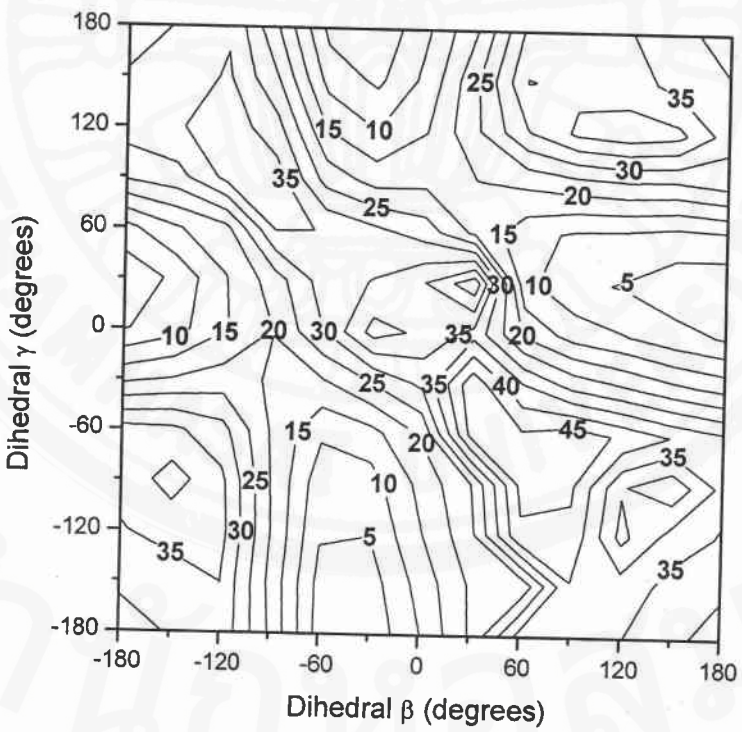

Figure 3.7 Contour plot of the energy hypersurface of B2HPM defined by the dihedral angles β and γ; the absolute energy minimum is set to zero, the energy difference between the individual contour lines is 5 kJ/mol.

In conclusion, FTIR spectroscopic results from solid phase and in dilute solutions of phenolic analogues of phenolic resins are examined. The results revealed that intramolecular hydrogen bonding formation between the two adjacent hydroxyl groups in B2HPM is responsible for a formation of lowest energy structural conformation suggested by structural analysis, and leads to an induction of intermolecular hydrogen bonding formation to generate "dimmer" or "trimer" B2HPM structures in dilute solution. The three infrared bands observed in the OH-stretching region of the compound's dilute solutions are therefore assigned to free, intra-molecular, and intermolecular hydrogen bonded OH, respectively. On the other hand, the corresponding results found in B4HPM suggested that a formation of similar hydrogen bonding is unlikely due to the separation of hydroxyl groups by its non-polar phenolic ring. The results obtained from these analogues can be used to explain the corresponding phenomena observed in the linear PCF resin, and the branch-structured phenolic resin, respectively.